UNIVERSITAT POLITÈCNICA DE CATALUNYA
BARCELONATECH
Escola Superior d'Enginyeries Industrial, Aeroespacial i Audiovisual de Terrassa

Bachelor's Degree in Aerospace Technology Engineering

Bachelor Thesis - Document: REPORT

Project of designing and manufacturing a small wind turbine using fused deposition modeling technology

Director:

Francesc Xavier Sanz Cano

Co-Director:

Álvaro Luna Alloza

Autor:

Guillem Vergés i Plaza

Delivery date: 00-00-0000

Presentation date: 28-10-2018

Abstract

Declaration of honour

Contents

List of Figures

List of Tables

Symbols

Symbol	Description	Unit
a	Axial induction factor	-
a'	Tangencial induction factor	-
C_d	Sectional drag coefficient	-
C_l	Sectional lift coefficient	-
C_P	Power coefficient	-
C_Q	Torque coefficient	-
C_T	Thrust coefficient	-
C_x	Coefficient of sectional blade element force normal to the rotor plane	-
C_y	Coefficient of sectional blade element force parallel to the rotor plane	-
Q	Torque	$\mathrm{N\,m}$
r	Local radius of the blades	m
R	Total radius of the blades	m
U_∞	Wind speed	$\mathrm{m\,s^{-1}}$
α	Angle of attack	rad
α_{opt}	Angle of attack - optimal	rad
α_s	Angle of attack - stall	rad
β	Geometric twist plus pitch offset of the blades	rad
λ	Tip speed ratio	-
λ_r	Tip speed ratio - local	-
ρ	Air density	$\mathrm{kg\,m^{-3}}$
σ_r	Local blade solidity	-
μ	Adimensional local radius of the blades r/R	-
τ	Geometric twist of the blades	rad
ϕ	Flow angle	rad
Ω	Rotor speed	$\mathrm{rad\,s^{-1}}$

Chapter 1

Introduction

1.1 Aim

1.2 Scope

1.3 Requirements

1.4 Justification of the need

Chapter 2

Development

2.1 Background and review of the state of the art

As the aim of the project is to design a new product, a good knowledge of the state of the art is necessary to have a starting point. In this section the current framework of small wind turbines will be described.

2.1.1 History and impact of small wind turbines

The first steps in the development of small and micro wind turbines took place during the thirties, with the objective of charging batteries in remote households. Manufacturers like Jacobs [1] or Parris-Dunn [2] produced this type of wind turbines in the United States. In the late forties, with the arrival of the electrical grid to the rural areas, this industry practically disappeared. It remained in hibernation until the seventies, when the petrol crisis created the need for alternative energy sources. Tha attention came back to the small wind turbine energy, not only in the United States but also in Europe, where, for example, the Bornay brothers started their company in Spain [3].

During the eighties this technology started to evolve, as the manufacturers began to abandon the DC dynamo generators and incorporated synchronous generators with permanent magnets (AC). In order to obtain a DC current for charging batteries, rectifiers were needed. Over time these rectifiers were connected to inverters to be able to connect the wind turbines to the grid. Induction generators began to be used as well in order to connect them directly to the grid, but it was a difficult solution to implement in isolated applications due to the generator's need to be excited from outside. The need for a gearbox also difficulted its success.The size and power produced started growing gradually, and before the ending of the eighties 50kW was considered a small wind turbine, with diameters of more than 15m. [4] The current regulations (IEC 61400-2 [5]) establish that the limit of a small wind turbine is given by a swept area smaller than 200m^2.

The small wind turbines technology has been evolving from the isolated applications to he modern grid-connected installations, and has even entered into the residential and urban outline. These last applications have caused the increased use of vertical axis solutions. The most well known developments are the Savonius and Darrenius wind turbines, but also the Gorlov design and some combined schemes are being used. [4]

Regarding the impact of the small wind energy, the last World Wind Energy Association

(WWEA) report indicates, from 2014 data, that there were 945,000 small wind turbines installed all over the world, producing almost 850MW. China and USA are clearly leading this market, and the biggest market in Europe is in the UK. Unfortunately, developing countries have an anecdotal presence, even though this was a technology initially developed with the objective of electrifying isolated regions, and the enormous wind power potential (especially in the eastern highlands of Africa) . All of this can be seen in the following figure:

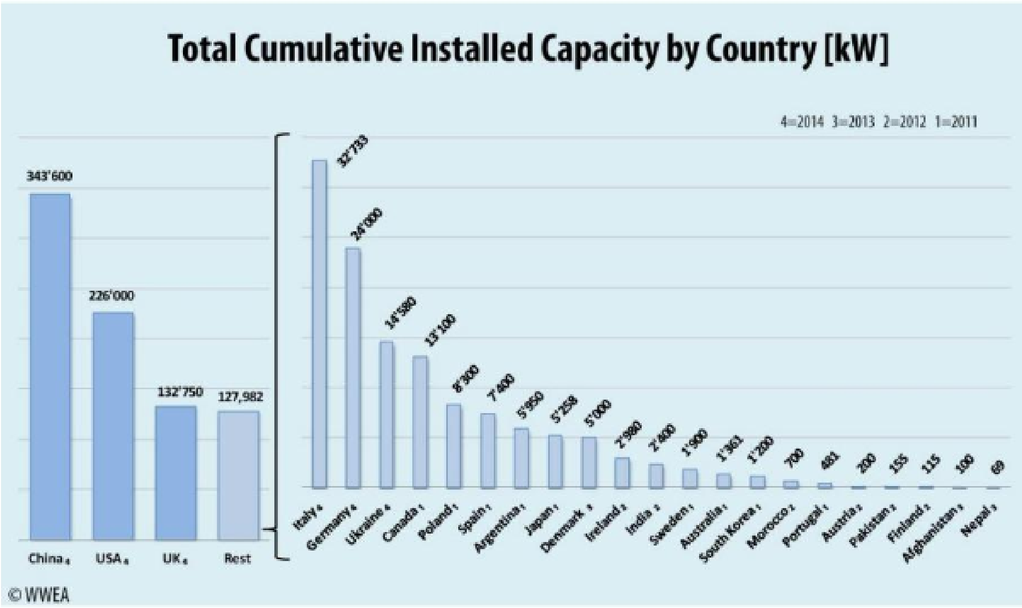

Figure 1: Total cumulative installed capacity of SWT by country.
Obtained from WWEA 2016 report.

The forecast for new installations in this report predicted a big growth in the annual installed capacity. Unfortunately there is no data available or a newer WWEA report to check the last tendency of the market.

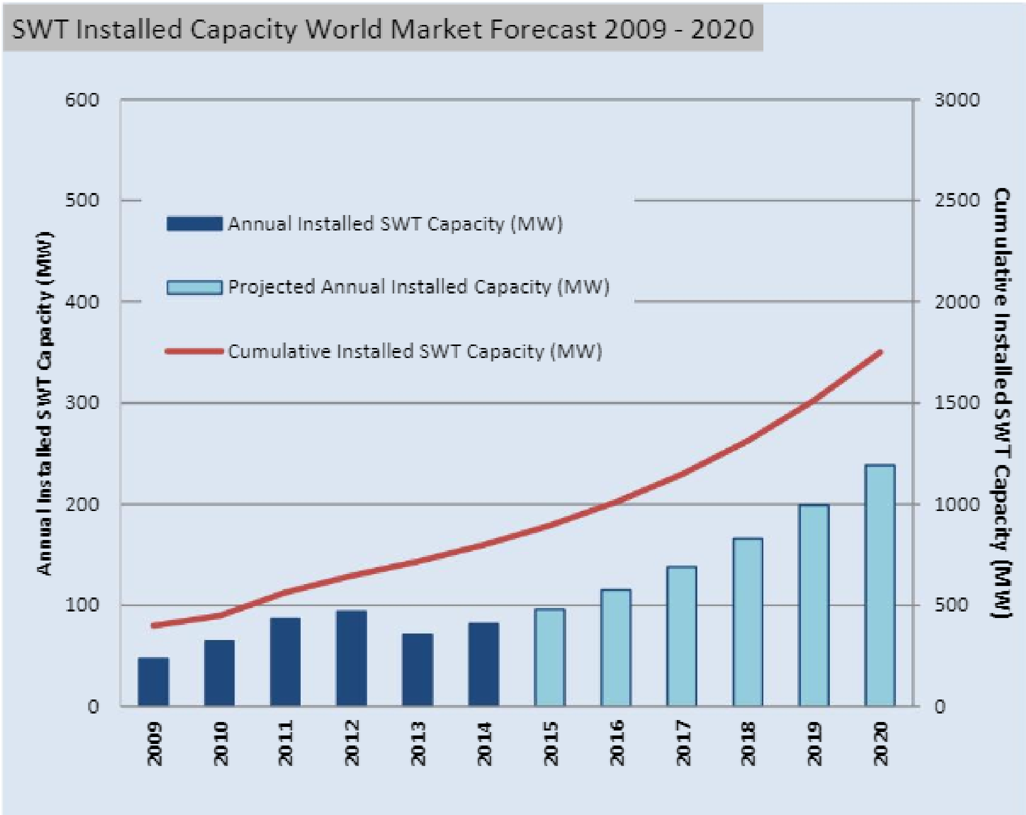

Figure 2: Small Wind Turbines installed capacity forecast.
Obtained from WWEA 2016 report.

Analyzing the perspectives in Spain, the last Renewal Energy Plan (PER) established the objective of reaching 300MW installed in 2020, predicting more than 50MW of new installations every year on from 2020. [6]

The investment in this kind of wind turbines is usually made by private individuals or small communities in order to partially or totally fulfill their demand for electricity or heating. However, a large portion of the buyers is disappointed by the actual energy obtained from these wind turbines. The main reason for this is the promotion of inaccurate and overstated information of the power output by manufacturers or installers. The satisfaction and reviews of this kind of products can spread very fast, and this type of feedback is reducing the confidence of this sort of economic investing, consequently slowing down this sector's growth. [7]

2.1.2 Advantages and disadvantages

The generation of electricity through small wind turbines has some particular advantages and disadvantages in comparison to larger wind turbines or other sources of renewable energy. In this section these particular characteristics will be enumerated. [4] [8]

Advantages

1. **Renewable energy**: It is virtually inexhaustible and does not produce air emissions nor pollution.

2. It can **coexist** with other installations and land uses (for example agriculture).

3. Easy and fast **installation**: the study made in section 2.1.4 shows that a strong point of commercial SWTs is the possibility of an easy installation, which facilitates direct sale to the final user.

4. Suitable for **isolated areas** due to the possibility of battery charging applications and integration with other types of generation. It allows the possibility to achieve electric energy independence.

5. Energy is generated close to the consumption points, which reduces the **transportation losses**. It also does not require additional big installations for transportation and evacuation of electricity.

6. **Reduced maintenance and operation costs**, and high reliability.

7. Less **environmental** and **visual impact**.

8. Can be generally optimized for **moderated wind speeds**, which eliminates the need for complex viability studies and allows a better production in average installation sites.

Disadvantages

1. The wind is intermittent, uncontrollable and relatively unpredictable, so **other sources of energy are required** to ensure enough electricity production.

2. The **visual impact** can still be a drawback.

3. The **noise** is important in residential areas.

4. **Flickering**: visual phenomena produced by the periodic projection of the blades shadow.

5. **Lack of complex active control systems** due to price limitations. SWTs are generally simpler than large wind turbines.

2.1.3 Design solutions

The design of any wind turbine in general has multiple options and solutions. In this and the following section these alternatives will be analyzed, first with an explanation of each solution and then with its presence and importance in the market. The main different approaches for small wind turbines will be explained below: the axis orientation (horizontal axis wind turbines (HAWTs) and vertical axis wind turbines (VAWTs)), the rotor position in relation to the tower (upwind and downwind), the addition of a duct (diffusor augmented wind turbines DAWTs), the number of blades and the power control.

Axis orientation

The major classification of wind turbines is commonly made from the position of the rotor axis of revolution: HAWTs and VAWTs. The most used solution is the horizontal design. As the small wind energy world usually follows the developments of the large wind turbines industry, close to 75% of SWTs are HAWTs. However, VAWTs have some advantages: they are conceptually simpler (since they do not require a yawing mechanism), there are some structural and maintenance benefits (the generator and the gearbox are placed close to the ground), and they need a lower cut-in wind speed. VAWTs can be based on drag (Savonius) or on lift (Darrenius), which is a much more efficient approach. A lot a of research is being done in the latter, as the aerodynamics are much more complex than HAWTs, and the overall performance is growing. VAWTs have been gaining presence in the last years, especially in urban environments. [9] [7]

Rotor position

The wind turbines can also be divided by the position of the rotor in relation to the tower. The most common solution is using upwind wind turbines, situating the blades (relatively to the wind) in front of the tower (windward). The other alternative is called downwind, where the rotor is located on the back side of the turbine.

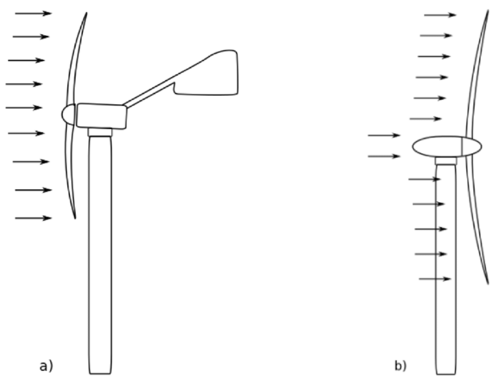

Figure 3: Upwind (a) and downwind (b) wind turbines.
Extracted from [7].

The upwind wind turbines are characterized by a higher efficiency, as the impact of the tower and the nacelle to the incoming wind is much smaller in this configuration. However, there is risk of collision between the rotor and the tower, so the blades are required to have a higher stiffness or either be placed with some angle or distance. Another drawback of this design is the need of a yaw system in order to keep the rotor facing the wind, as the natural trend of the rotor is to move to the downwind position. In the SWTs this is usually accomplished using a tail vane.

These special requirements of the upwind wind turbines are precisely one of the principal advantages of the downwind design: they are simpler. The lack of these needs is also beneficial in regard to the structural dynamics and weight of the wind turbine. The main disadvantage is the influence of the tower and the nacelle to the incoming wind profile, which leads to fluctuations of momentum in the blades. The fatigue damage and the resonance risk are a real danger to take into account. The noise generated is higher, as the turbulence produced by the tower will impact the blades. [7]

Diffusor augmented wind turbines

An innovative design for HAWTs is the usage of a circular duct that encapsulates the rotor. These wind turbines are called DAWT, compact wind acceleration turbine (CWAT) or wind lens. The objective of this solution is to accelerate and uniformize the incoming flow through the rotor. Some studies have shown in wind tunnel test the benefits of this system [10], but little results are obtained in real outside conditions. The added mass due to the diffusor puts more stress in the tower and makes the operation of the yaw system more difficult. However, it is not strange to see this kind of system in boat's SWTs. [7]

Number of blades

The selection of the number of blades (only referring to HAWTs) is a compromise between different aspects. The effects of varying the number of blades can be analyzed from both an aerodynamic and a dynamic perspective.

From the aerodynamic point of view, the performance (power coefficient) increases with the number of blades, but this effect has less importance from 3 blades on. The optimal rotational speed, on the other hand, decreases with the number of blades, and this is important to take into account because the aerodynamic noise produced (the most predominant) scales with the fifth power of the blade tip speed.

From the dynamic point of view, the main goal is to reduce the rotating mass in order to diminish the loads that the structure will have to support. The weight of each blade is important.

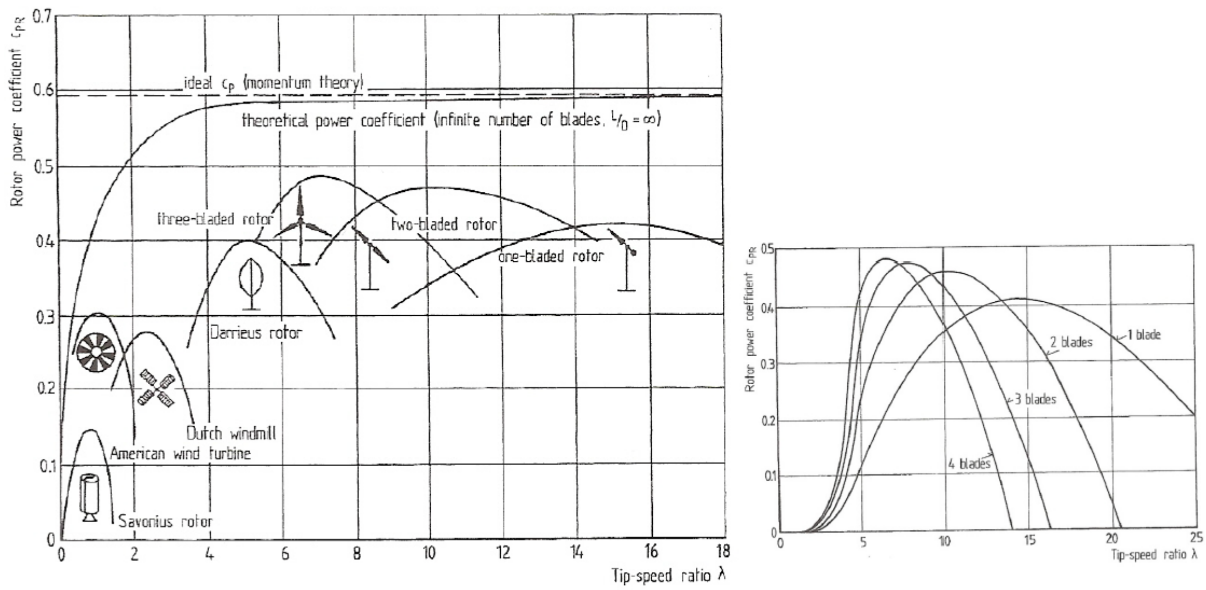

Figure 4: Power coefficient as a function of the number of blades and wind turbine type. Extracted from [8].

The dominant solution for multi-megawatts wind turbines is the three-bladed rotor. More variety is observed in the world of SWTs, but the most used design is composed of three blades as well. The main advantage of this design is a higher stability: the power output oscillates less during a turn, the gravitational and gyroscopic forces are better balanced (reduction of vibration problems), and a smoother operation is achieved. The noise and the visual impact are also reduced. However, they are heavier and more complex in general than two or one-bladed rotors, and the installation and control system are more complicated. [8]

Power control

Once the generator reaches nominal power, a control system is required in order to maintain this value. This control system is also necessary to protect the wind turbine in case of stronger winds. If the wind speed exceeds the one required to reach nominal power, this system will waste part of the excess energy in order to avoid damaging the wind turbine. This is achieved, typically, by either an active pitch control or a passive stall control.

In a passive stall control system, the blades are bolted onto the hub at a fixed angle. As the actual angle of attack of the blades increases with the wind speed, the fixed pitch and twist of the blade can be designed in order to get the blades to stall at a desired point. If the rotor stalls, the torque and power generated will diminish. This solution avoids the need of a complex variable pitch system, but higher loads will be experienced, and an aerodynamic brake will be required.

On a pitch controlled wind turbine, there is an electronic controller that receives the generator's power output. If this magnitude becomes excessively high, the controller varies the pitch of the blades. The effective angle of attack is reduced, and the torque and power produced by the blades drop. [11]

2.1.4 State of the market

The table 1 indicates a sample of the small wind turbines that can be commonly found in the market nowadays. Some interesting conclusions can be extracted from it:

1. The dominant design is the **horizontal axis wind turbine**, as seen in the preceding section.
2. All of them use **direct drive** configuration (lack of gearbox).
3. All mention a **low start torque** resulting in a low start wind speed (between 2 m/s and 4 m/s). However, it has been seen that the power output at these wind speeds is also very low. The objective of this feature could be an automatic starting procedure.
4. The usage of **UV protection coatings** on the blades.
5. The **installability** and the **low noise production** are essential characteristics from a commercial point of view.
6. Almost all of them are configured for **battery charging applications**, and some of them have one version for grid connexion and another one for battery charging at 24/48 V.
7. Most of them require a **tower** of at least 10 m height to reach nominal power (by manufacturer indication). However, almost none of them include it. Some brands offer the tower separately from the wind turbine, which is sold at almost the same prize as the wind turbine itself.

Table 1: State of the market of small wind turbines.

Manufacturer and Model	Architecture	Number of blades	Rotor diameter [m]	RPM	Nominal wind speed [m/s]	Nominal power [W]	Material	Control system	Generator	Weight [kg]
Bornay 13 [3]	HAWT, Upwind	2	2.86	@600	12	1500	Carbon or glass fiber	Electronic regulator and pasive by inclination	Trifasic with permanent Neodymium magnets	41
Bornay Bee 800 [3]	HAWT, Upwind	5	1.75	@500	12	800	Injected nylon	Electronic controller	Trifasic with permanent Neodymium magnets	29
Enair E30 PRO [12]	HAWT, Upwind, self regulating	3	3.80	250	11	1900	Glass fiber	Passive pitch control with two action speeds	Neodymium permanent magets (30 poles)	125
SD Wind Energy SD3 [13]	HAWT, Downwind, self regulating	3	3.90	Màx 300	-	3000	Glass Thermo-plastic Compos-ite	Passive	Brushless permanent magnets	-
Smarttwister ST-1000 [14]	VAWT, Helicoidal blade	1	0.34 (1.38m height)	525	7.6	1000	Technic nylon	Electronic controller	Neodymium permanent magnets	34
Aeolos V 300W [15]	VAWT	3	1.20 (1.60m height)	300	10	300	Aluminum alloy	-	Permanent magnets	10
Bergey Excel 1 [16]	HAWT, Upwind, self regulating	3	2.50	-	11	1000	Glass fieber	Furling against high wind speeds	Neodymium permanent magets	34
AutoMaxx DB-400 [17]	HAWT, Upwind	3	1.22	-	13	400	Nylon and glass fiber	Electronic controller	Brushless permanent magnets	10
MarsRock 400W Economy Windmill [18]	HAWT, Upwind	3	1.40	400	13	400	Nylon and glass fiber	Electronic controller	Trifasic with permanent magnets	10

2.2 Approach and decision on possible solutions

In this section, the design approach that will be followed is discussed and justified.

2.2.1 General architecture

The general architecture of the wind turbine will be based on the tendencies seen in the state of the market.

1. **Horizontal axis, upwind wind turbine:** The horizontal axis option is selected because it is the most used and studied. Although the vertical axis is growing in importance, the classic concept will be chosen. The rotor position will also follow the usual convention: an upwind wind turbine will be selected. A downwind concept would simplify the yaw stabilization system, but it could also lead to big fatigue loads and dangerous aeroelastic coupling. As the loads analysis that will be performed does not involve a detailed aerolastic temporal analysis, it is desirable to avoid this possible problems since the beginning.

2. **Three blades:** In the figure 4 the influence of the number of blades on the optimal tip speed ratio and maximum power coefficient has been shown. Following the same reasoning that was discussed there, it is desirable to increase the power coefficient by selecting a higher number of blades, but the cost in material and forces of this option are the main drawback. In a small wind turbine, the effect of the tip speed ratio should be taken into account. Because of the small radius, if a high tip speed ratio is desired, the angular velocity of the blades should be very high. Thus, the corresponding centrifugal forces will increase as well. An approximated magnitude of this effect is represented in the following figure:

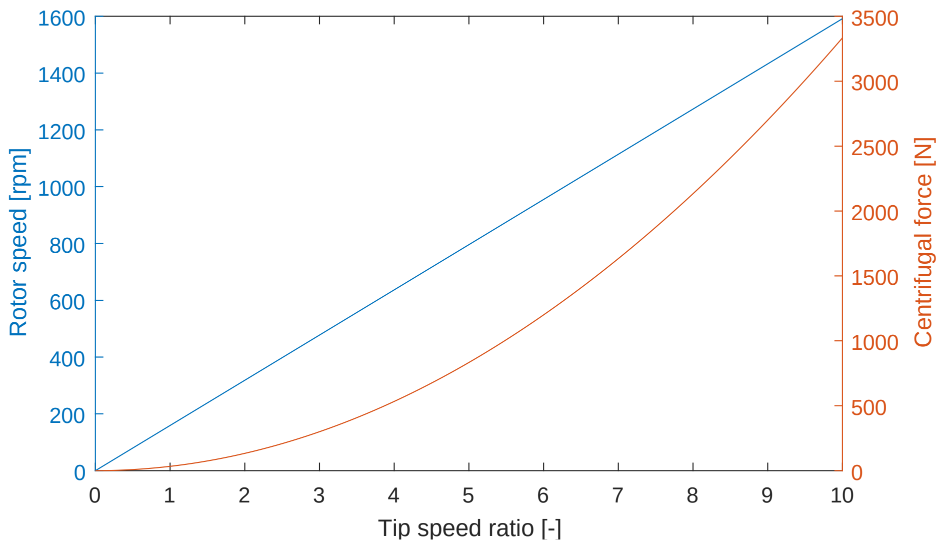

Figure 5: Influence of the tip speed ratio on the centrifugal force.
Values estimated at 10 m/s for a wind turbine of 1.2 m diameter.

This illustrates the importance of being able to operate at the lower tip speed ratio possible. This is why three blades are preferable rather than two, specially in this case. When it comes to change from three to four blades, the decision is not that clear. The increase in power coefficient and the decrease in rotor speed are lower, and the rotor instability might be a source of problems. The hub design is also compromised (more blades to join, more space needed), and the blade cost is increased again. Thus, this option is discarded and three blades will be the final choice, following the trend of the market.

3. **1.0 m rotor diameter:** The rotor diameter selection is constrained by the possibilities of the 3D printer that will be used. The printer characteristics will be exposed more deeply in the section 2.5.1.1. The biggest restriction that it imposes is the available printing space: 220x220x250 mm, which means that the blades will have to be built out of more than one piece. It can be anticipated that the join between the different parts will be an added difficulty to the design, so it may be helpful to reduce the amount of parts. A blade made of two pieces is selected. This option will keep the material cost as low as possible but will still involve the challenge of joining two different parts, and the study and methodology used could be extrapolated to even more parts.

   For the first design, it will be assumed that each piece will be 25 cm long, so the blade radius will be 50 cm. However, this assumption neglects the presence of the hub, which would "add" diameter, and also ignores any radial extra space used for the joint, what would "subtract" diameter.

4. **Entirely passive control system:** Large commercial wind turbines count with torque and pitch control systems, which allows them to reduce loads, have a big range of operation capabilities and ultimately increase the power production. On the other hand, small wind turbines seldom have a pitch controller, and the torque controller is not a clearly dominant option. For this project, none of them will be developed.

   Although a torque controller would simplify the aerodynamic design (as the rotor speed could be practically selected for each wind speed), there are two major drawbacks. First, the hardware would increase in cost (a different generator plus the variable speed drive) and the software would increase in complexity. Second, it is desirable to come up with a design that can be easily reproduced for anyone with access to a 3D printer. If a control system is included, with both the hardware and software it involves, it will be likely more difficult to replicate.

5. **Over-speed control by furling:** This characteristic is highly related to the preceding one. An over-speed control is needed even though there is not any controller for the normal operation. This will allow the turbine to operate safely under extreme wind conditions, which will increase its life span and simplify the structural requirements. There are two main options for a passive over-speed control:

   The first option is a furling mechanism, which turns the rotor away from the incoming wind flow. The rotor can be either rotated around the tower axis or around the axis perpendicular to the tower and contained in the rotor plane. This rotation is achieved through the higher thrust obtained at higher wind speeds, and the system should be designed in a way that this higher force creates a moment around the above-mentioned axis. The furling mechanism should be dimensioned so that the deviation occurs at the desired wind speed.

The second option is a passive stall mechanism, which simply uses the reduction in lift coefficient and the increase in drag coefficient in the post-stall region to create a ceiling in the power level as the wind speed increases.

The passive stall mechanism is a simpler option. However, it imposes big restrictions in the blade geometry, and it creates big uncertainties in the aerodynamic post-stall behavior. Most importantly, it is a requirement for applying this option that the angle of attack increases with the wind speed. In the section 2.4.2.2 it can be seen that this is not meet. Due to all these disadvantages, a furling mechanism is selected.

6. **Direct drive:** In the state of the market it has been seen that the tendency of the market is to avoid the use of gearbox, which adds weight, mechanical complication and decreases the efficiency. This preference will also be followed for this project.

7. **Permanent magnet generator:** Again, the market standard will be followed to select the generator type.

2.2.2 Design procedure

In a wind turbine almost everything is coupled. Therefore, is difficult to separate and design each part separately. To obtain a complete design that takes into account all the different parts, a iterative process should be made. The following figure shows the procedure that will be followed, as well as the different parts where the design can be divided into.

2.3 Electric design

2.3.1 Introduction and general architecture

2.3.2 Generator selection

2.4 Aerodynamic design

2.4.1 Airfoil selection

In this section, the selection of the airfoils for the blades will be made. First, the desired characteristics will be defined. The low Reynolds influence will be described, and a study methodology will be chosen according to it. Then, several existing airfoils will be selected to be studied and a selection criteria will be detailed.Finally, the elected airfoil will be characterized.

Desired characteristics

The desired performance of the blades varies from root to tip. The optimal solution would be to have blades with aerodynamic twist and adapt the airfoil selection to the different circumstances of each section of the blade. However, this would difficult the optimization of the chord and geometric twist distribution, so only one airfoil will be selected.

This selection is a compromise between aerodynamic and structural issues. Usually, a high relative thickness is used at the root (around 35%) and a lower one at the tip (18%). The biggest drawback of a single-airfoil blade is that this could not be done. The desired characteristics of the airfoil are enumerated in the following list: [8] [19]

1. Good performance at low Reynolds number.
2. High efficiency $(C_l/C_d)_{max}$.
3. Margin between optimal and critical conditions (stall angle of attack far from the optimal angle of attack to be resistant to perturbations)
4. High lift coefficient: a higher lift coefficient would lead to a lower chord, resulting in less loads and costs.
5. Soft stall behaviour.
6. Insensitive to dirt (turbulent airfoils are more resistant).

Low Reynolds number and simulation parameters

The Reynolds number in a small wind turbine is defined as:

$$Re = \frac{\rho U_T c}{\mu} \tag{1}$$

Where U_T is the "total" velocity at the blade, c is the chord, ρ is the air density and μ the dynamic viscosity. Note that the first two variables change along the blade. Note that the lower Reynolds value will be achieved when the blades are stationary and $U_T = U_0$. The typical Re ranges for small wind turbines and other aerodynamic bodies can be found in the following table:

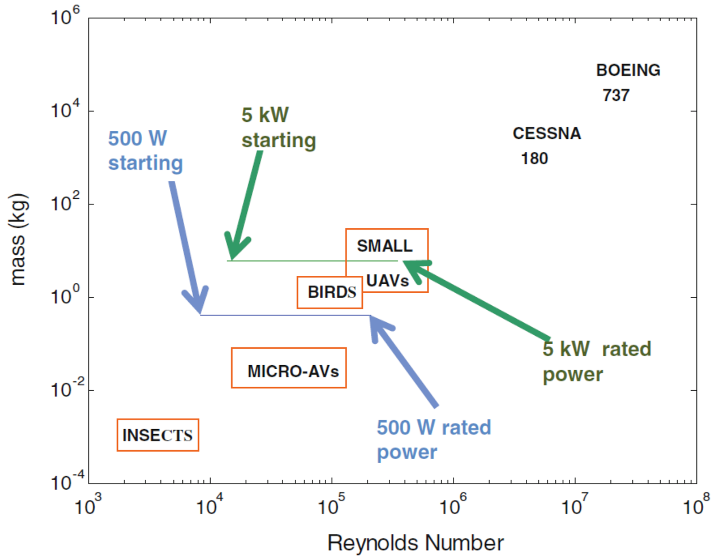

Figure 6: Reynolds number ranges for small wind turbines and other aerodynamic bodies. Obtained from [19].

The airfoils will be studied using XFOIL sofware with XFLR5 graphical user interface. As it uses an inviscid linear-vorticity panel method with a Karman-Tsien compressibility correction, this software shows reliable results for low Re flows. Note that it was initially intended for the calculation of model sailplanes. The following constant parameters need to be defined to set up the simulation [20]:

1. **Mach number**: As XFOIL considers incompressible flow (M=0) any value below 0.3, this value is initially defined as $M = 0$.

2. **Boundary layer transition**: It is assumed that the laminar to turbulent transition will occur due to the roughness of the blades. The XFOIL documentation is followed, and a value of Ncrit = 1 is set. [21]

3. **Reynolds number**: Although reliability can be expected from XFOIL results, the error increases at significant low Reynolds. The following Reynolds will be studied: $Re = 2 \cdot 10^5$, $Re = 1.6 \cdot 10^5$, $Re = 1.2 \cdot 10^5$, $Re = 8 \cdot 10^4$, and $Re = 4 \cdot 10^4$.

Airfoils studied

The following table summarizes the airfoils that will be tested and studied. The airfoil coordinates and the values presented below has been obtained from *airfoiltools.com* [22], a useful website that uses UIUC's airfoil database [23]. All the airfoils studied have been designed looking for a good performance in low Reynolds number operation. Some of them are specifically designed for small wind turbines: SG series (Selig-Giguere) and S833/4/5 airfoils designed by NREL are probably the first aerofoils designed for this purpose [19]. The other models have been selected by looking into low Reynolds airfoils studies [20] [24].

Table 2: Airfoils selected to be studied. All values are indicated in chord percentage.

Code	Airfoil	Maximum thickness [%]	Position [%]	Maximum camber [%]	Position [%]
1	SG6040	16.0	35.3	2.3	60.5
2	SG6041	10.0	34.9	1.5	49.7
3	SG6042	10.0	33.5	3.3	51.5
4	SG6043	10.0	32.1	5.1	53.3
5	S833	18.0	36.3	2.5	78.8
6	S834	15.0	39.5	1.6	60.0
7	S835	21.0	30.5	2.4	78.0
8	S1210	12.0	21.4	6.7	51.1
9	S1223	12.1	19.8	8.1	49.9
10	S6063	7.0	29.4	1.3	43.8
11	S9037	9.0	28.5	3.3	42.4
12	S3010	10.3	25	2.3	43.3
13	SD8000	8.9	29.4	1.5	54
14	BW3	5.0	7.4	5.7	45.4
15	E387	9.1	31.1	3.2	44.8
16	E374	10.9	34.3	2.0	38.9
17	E62	5.6	26.2	5.0	49.3
18	RG15	8.9	30.2	1.8	39.7

The following parameters will be analyzed for each airfoil:

1. Maximum efficiency E: An airfoil that produces the more lift possible with the minimum drag is desired.
2. $\Delta\alpha = \alpha_s - \alpha_{opt}$: It is important to have the optimum angle of attack far from the stall angle of attack, as this provides consistency to the design.
3. $\frac{d\alpha_{opt}}{dRe}$: The Reynolds range that the airfoil will work at makes desirable to have uniformity in the optimal operating point. Hence, the lower variation of its location is searched.
4. $\frac{dE}{dRe}$: The same reason than the previous point.
5. $\frac{dE}{d\alpha}(\alpha = \alpha_{opt})$: This parameter is also studied in order to provide consistency. Variations of α should not lead to huge changes in the efficiency.
6. Thickness t/c: The thicker the airfoil, the more structural resistance it has. Usually the thicnkess is a compromise between the aerodynamic performance and the structural perspective.
7. Cl_{opt}: The higher the lift coefficient for, the smaller the chord needed.

An explanation of how the data have been extracted from each airfoil can be found in the section 1.1 of the Report Attachment. The polar curves and data from each airfoil is also presented there with more detail. The results are summarized in the following table:

Table 3: Airfoil selection results.

Nº	Airfoil	Parameters						
		1	2	3	4	5	6	7
		E_{max}	$\alpha_s - \alpha_{opt}$	$d\alpha_{opt}/dRe$	dE/dRe	$dE/d\alpha$	$(t/c)_{max}$	Cl_{opt}
1	SG6040	44.11	10.81	0.55	9.86	4.66	16.00	0.87
2	SG6041	42.46	6.02	0.36	7.50	2.14	10.00	0.89
3	SG6042	48.89	9.24	0.64	8.01	2.57	10.00	0.85
4	SG6043	57.73	10.96	0.94	11.87	5.59	10.00	0.97
5	S833	31.13	8.59	0.69	6.32	1.32	18.00	0.75
6	S834	32.30	7.62	0.33	5.96	1.32	15.00	0.69
7	S835	27.96	10.03	0.60	6.00	1.97	21.00	0.67
8	S1210	62.47	6.32	0.31	12.13	4.80	12.00	1.40
9	S1223	55.67	5.63	0.37	10.55	1.44	12.10	1.52
10	S6063	36.78	3.89	0.18	5.36	5.57	7.00	0.67
11	S9037	50.95	6.57	0.09	8.55	2.33	9.00	0.93
12	S3010	48.35	5.97	0.07	8.59	2.45	10.30	0.94
13	SD8000	42.76	5.35	0.06	7.24	2.15	8.90	0.84
14	BW3	45.99	6.27	0.49	5.89	2.96	5.00	1.08
15	E387	56.17	6.85	0.66	10.42	9.22	9.10	0.89
16	E374	44.81	7.98	0.56	7.04	6.69	10.90	0.71
17	E62	65.55	7.02	0.72	11.70	13.64	5.60	0.95
18	RG15	43.48	5.41	0.25	6.74	4.66	8.90	1.83

In order to select which airfoil will be used, the preceding table should be normalized, and each parameter should have a weight assigned. A common risk when comparing different possibilities is to select an option which stands out in a particular variable but is not the best option in average. To avoid so, a domination matrix will be used [25]. The matrices with normalization and the domination procedure may be found in the section 1.1.2 of the Report Attachment.

2.4.2 Blades design

In this section the whole aerodynamic design of the blades will be reviewed. Firstly, the method to compute the power curve of a given blade geometry will be described. After that, different methods to optimize it will be discussed, as well as the distinctive feature that this passive solution should take into account.

2.4.2.1 Power curve calculation

To be able to design the blade geometry, the first step is creating a code to obtain the power curve from a given chord, pitch and twist. These three will be the variables to be determined. With them, the goal is to maximize the Annual Energy Production (AEP) by means of the power curve.

If a generator is selected, the curve of torque vs rotor speed $Q = f(\Omega)$ is fixed. This curve will also be the one that the wind turbine will follow. With it, it is already know how much torque the rotor will have to produce at each rotational speed in order to match the generator demand and achieve an equilibrium point. The remaining task is to compute the at which wind speed these equilibrium points are obtained. If a $\Omega = f(U_\infty)$ function can be found, then these points can be traced into a $Q = f(U_\infty)$ function and the desired power curve $P = f(U_\infty)$ would be immediate to obtain. In order to do so, the following procedure has been made:

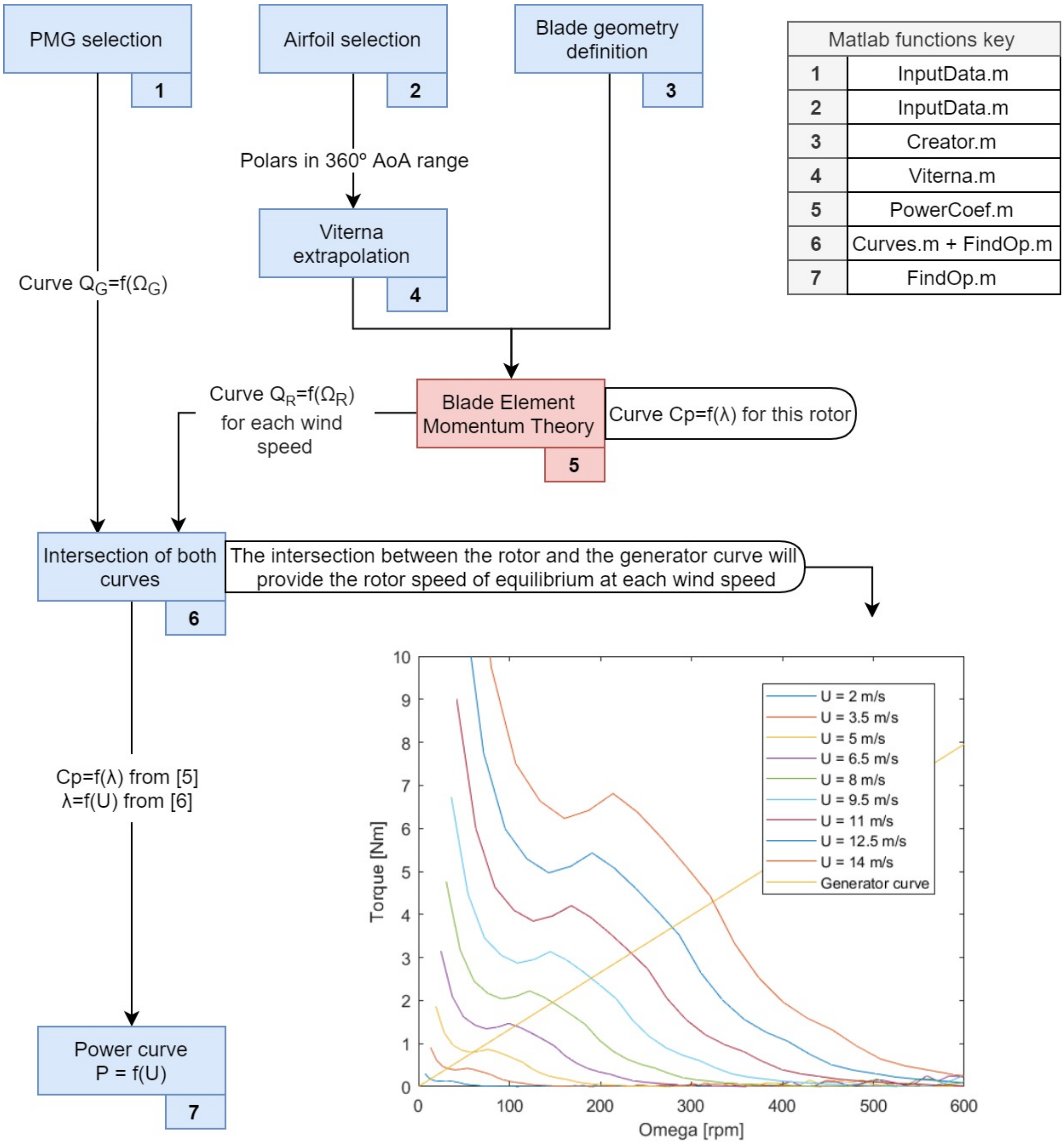

Matlab functions key	
1	InputData.m
2	InputData.m
3	Creator.m
4	Viterna.m
5	PowerCoef.m
6	Curves.m + FindOp.m
7	FindOp.m

Figure 7: Power curve calculation procedure. Includes the Matlab function created for each step, so the code is easier to analyze.

2.4.2.2 Initial approach and design challenge

A first study was carried out in order to see the general behavior of the wind turbine, analyze trends, and start to delimit which blade geometry may be more beneficial. To do so, a big number of chord and twist distributions were simulated. The pitch was also included, but as there is not any kind of pitch control, it is treated as a static offset to the twist.

The first consideration that should be taken into account is the fact that the wind turbine will be working at a very big RPM range. The generator has a nominal rotor speed of 600 RPM, whereas a typical commercial size wind turbine (e.g. General Electric - Cypress platform) works around 10 RPM. The dimensions of them are clearly not comparable, and the reference parameter should be the tip speed ratio. This will be the focus of this study and the source of the design challenge.

Both the chord and twist distribution used were obtained using the analytic formulas proposed in the section 3.7.3. of the Wind Energy Handbook by T. Burton et al. [9]. These expressions are analytically obtained in order to have the optimum induction coefficients a and a' (and thus, maximizing the power coefficient C_P) for a given tip speed ratio λ. For obtaining these formulas no losses have been taken into account. Moreover, the drag has been ignored, although it is demonstrated in the section 3.7.4. of the Handbook that the effect of including it is indeed negligible.

$$c = R\frac{2\pi}{\lambda N C_L}\frac{8/9}{\sqrt{4/9 + (\lambda\mu)^2 \cdot \left(1 + \frac{2}{9(\lambda\mu)^2}\right)^2}} \tag{2}$$

$$\beta = \phi - \alpha = \arctan\left(\frac{2/3}{\lambda\mu\left(1 + \frac{2}{9(\lambda\mu)^2}\right)}\right) - \alpha \tag{3}$$

The α is selected to get the maximum efficiency C_L/C_D, and the lift coefficient is given by it. For this step, this point is obtained with the average of all Reynolds number studied. The airfoil study showed that this airfoil has little angle of attack variation at different Reynolds numbers, so this selection is representative of all the operation region. For this study, different pitch variations (offset to the twist) have been applied.

To have a general sense of what the optimal blade geometry for this case will look like, the procedure shown in the preceding section has been applied to all the different chord and twist distributions. Then, the Annual Energy Production (AEP) has been calculated using a Weibull wind speed distribution. The Weibull used, due to the lack of experimental data of a possible installation site, corresponds to the reference one used in the Small Wind Turbine Contest [26]: $A = 4.5$ m/s ($V_{ave} = 4.0$ m/s) and $k = 2$. The blade geometry that lead to the higher AEP has been selected, and now its characteristics are going to be analyzed.

First, the chord and twist distribution of the selected blade geometry:

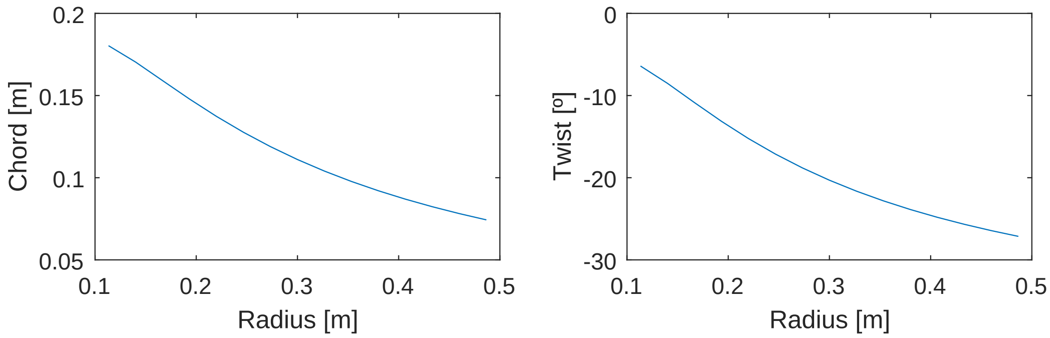

Figure 8: First chord and twist distribution obtained. This distribution is optimized for a tip speed ratio of 2.8, and has a pitch offset of -36º.

At first glance, it might seem abnormal the large pitch offset that is applied to the twist. The optimal twist distribution is created such that the effective angle of attack seen by the blades is always the optimal one α_{opt}. Therefore, a big change like that is surprising. The explanation of why this is more beneficial from an AEP point of view will be developed after the presentation of these first results.

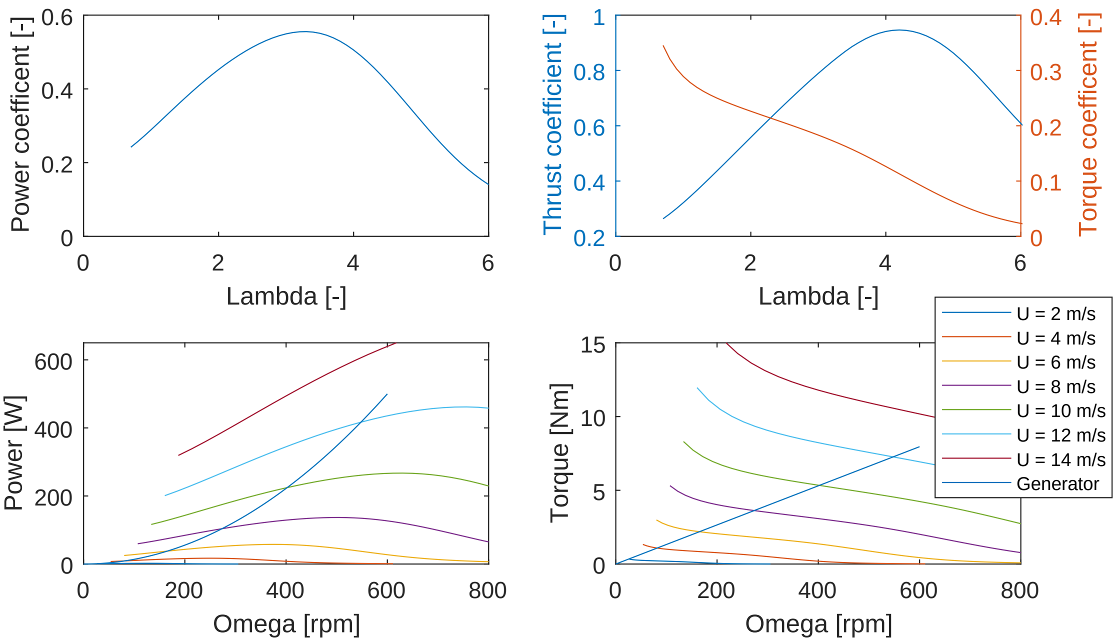

Figure 9: Rotor coefficients as a function of lambda and intersection with the generator curve. The bottom plots show both the generator (the curves that start at the origin of coordinates) and the rotor curves. The rotor curve is shown for different wind speeds and tip speed ratios. Each different curve is one wind speed, and each of its points corresponds to a different tip speed ratio.

As it was explained in the preceding section (Figure 7), the intersection of the rotor and the generator curve will give the operating points of the design. By doing so, the following power curve and operation are obtained.

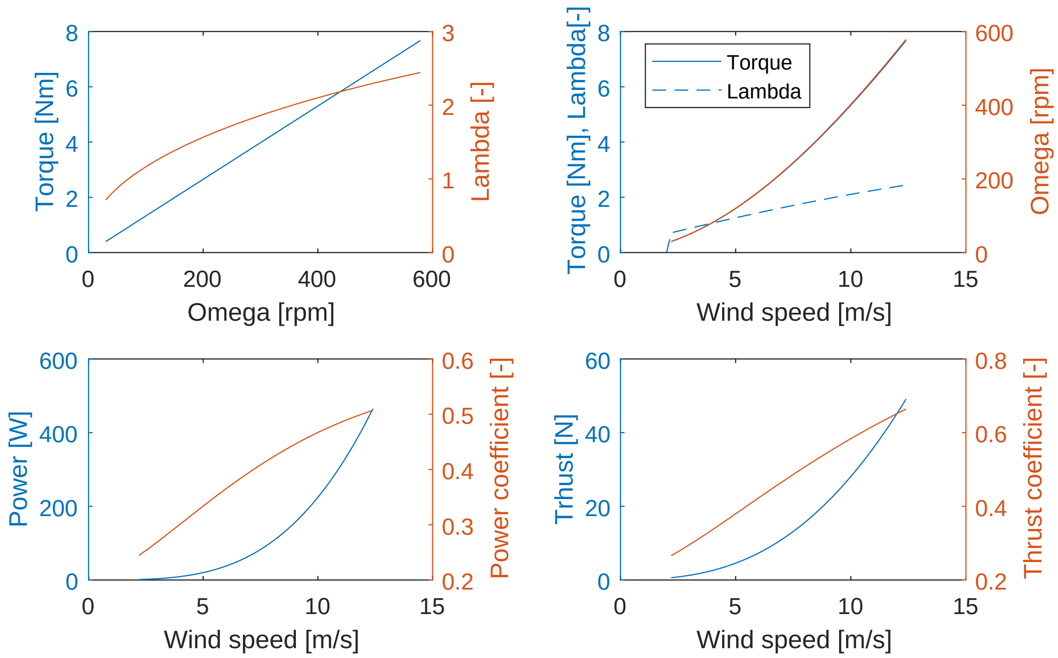

Figure 10: First operation results.

The cut-in wind speed is the one at which the power extracted by the blades is enough to energize the generator. On the other hand, the cut-out wind speed is the wind speed such that the maximum generator power is reached. The region after that will be treated separately, because it will involve furling and big yaw misalignment, and these phenomena is not easy to study with the BEM theory.

The most important remark about the results obtained may be seen in the top right plot. The dashed blue lines shows the tip speed ratio λ as function of the wind speed. Clearly there is a large variation from the cut-in (0.71) to the cut-out (2.44). It is interesting to note that this variation has been found not only in this design, but in all the different rotor geometries analyzed. This has an immediate effect on the angle of attack seen by the blades during all the operation. From the BEM (inherent definition of the induction factors) it is known that the angle of attack α can be obtained as follows:

$$\alpha = \phi - \beta = \arctan\left(\frac{U_\infty(1-a)}{\Omega r(1+a')}\right) - \beta = \arctan\left(\frac{(1-a)}{\lambda_r(1+a')}\right) - \beta \tag{4}$$

The inverse tangent is a growing function. Thus, if the tip speed ratio is increased, the fraction will decrease, and the angle of attack will decrease (as β, the sum of the twist and the pitch, is constant). This also depends on the induction factors a and a', but this explanation is enough to understand this effect, and the variation of these factors is more difficult to predict and study as they also depend on the tip speed ratio. The mean angle of attack as a function of the wind speed may be seen in the following figure.

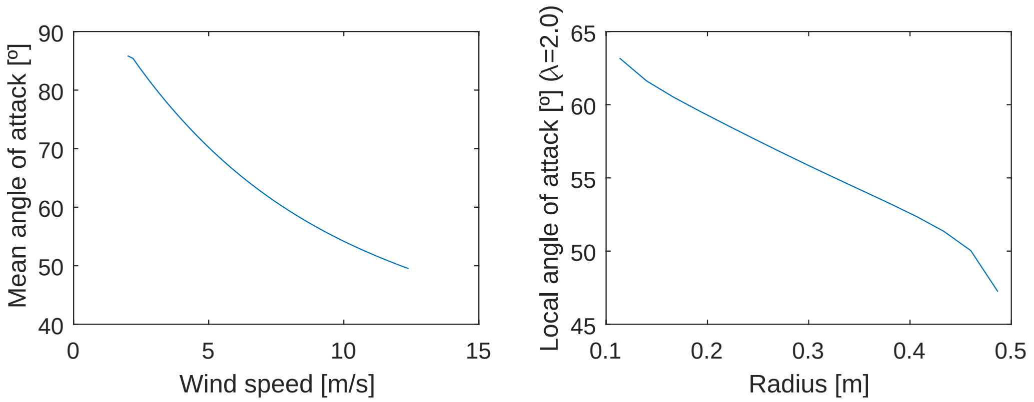

Figure 11: Angle of attack variation of the first results. The left plot shows the mean angle of attack (of all sections) as a function of the incoming wind speed. The right one shows the local angle of attack for a given tip speed ratio ($\lambda = 2$).

The large angle of attack variation anticipated is observed. The initial mean angle of attack is 85.6º, whereas at the cut-out wind speed is less than 50º. There is a change of more than 40º during all the operation curve. Then, the main question to be asked is: why a design like that appears to be the optimal one? It is surprising that the working region of the airfoils is outside the linear zone. In order to find out an explanation, the airfoil polar can be plotted once again:

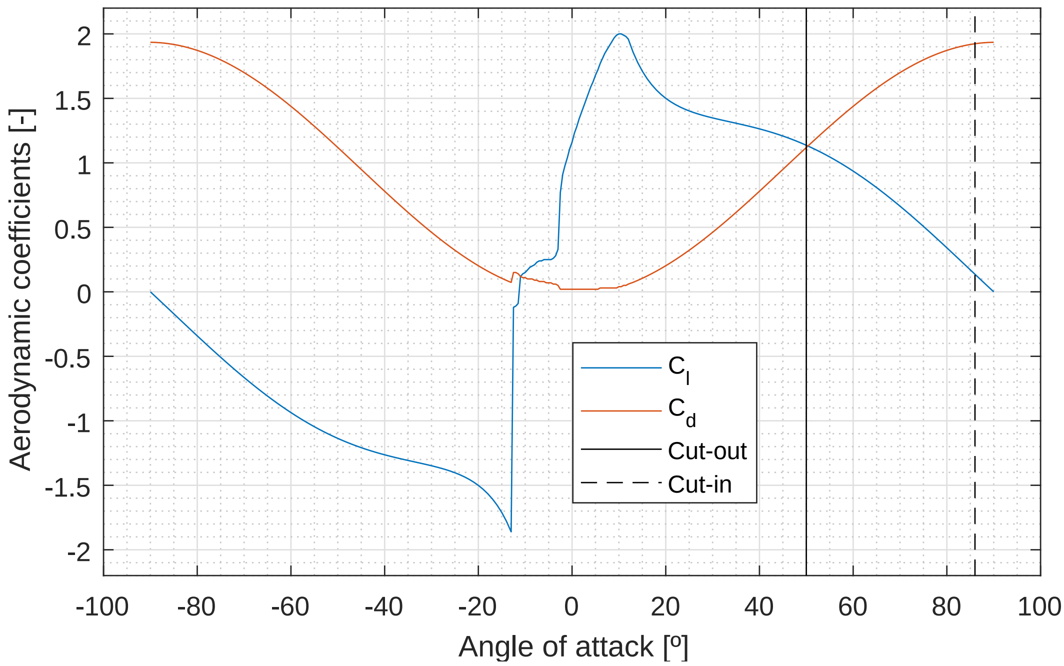

Figure 12: Airfoil polar with operation region indicated.

To understand why this operation is more beneficial, firstly it could be analyzed what would happen if the operation regime was located in the linear region. If the cut-in mean angle of attack were, for example, 20º, and the cut-out one were -20º, almost the half of the operation would have a negative lift coefficient. The BEM equations from which the axial induction factor is obtained may show the effect that this has:

$$C_l \cos\phi + C_d \sin\phi = C_x \tag{5}$$

$$\frac{a}{1-a} = \frac{\sigma_r}{4\sin^2\phi} C_x \tag{6}$$

The coefficient of sectional blade element force normal to the rotor plane C_x would be negative in that case, therefore the axial induction factor a would be less than zero as well. It should be constrained between 0 and 1, so this possibility cannot be studied with the BEM theory without reversing the rotational direction. It makes no sense to reverse the direction in the middle of the operation. Moreover, an operation like that would not match the generator curve, so it would not be possible.

On the other hand, if the operation is contained in the region obtained, the lift coefficient variation is more stable. Furthermore, its value near the cut-out region (where the power produced is higher) is also larger, which is an advantage from a power coefficient point of view. It could be argued that operating from 60º to 20º, for example, would be more beneficial, because the operation would be as solid as the obtained one, and the lift coefficient values would be higher. Firstly, the influence of the flow angle ϕ should be taken into account with more detail, and secondly, the number of blade geometries tested was low (225), so it is likely that no geometry capable to operate at that regime was created. Nevertheless, this first study was intended to understand the design challenge that will be faced, as well as the general operating characteristics of the design, and this result is enough for that.

An operation like this is not viable. The post stall region is very stochastic, unstable, and it could easily lead to high vibrations and aeroelastic instabilities. The drag is also unacceptable there. However, the behavior seen here is also obtained in other blade geometries analyzed, so it must be taken into consideration for further design. This performance could be summarized as follows: decrease of the angle of attack and increase of the tip speed ratio from the cut-in to the cut-out. It is also interesting to note that a stall control could not be implemented. A typical stall regulated wind turbine works in a constant rotor speed. As the tip speed ratio is defined as $\lambda = \Omega R/U_\infty$, as the wind speed increases, the tip speed ratio decreases, and it has been demonstrated that a lower tip speed ratio leads to a higher angle of attack. If it is design properly, the stall will be reached at the desired wind speed.

2.4.2.3 Optimization procedure

2.5 Structural design

2.5.1 3D printing previous considerations

2.5.1.1 Printer characteristics

2.5.1.2 Filament selection

2.5.2 Load cases

2.5.3 Link design and printing properties

Chapter 3

Summary of the results

3.1 Budget summary

3.2 Analysis and assessment of the environmental implications

3.3 Future lines of work

3.4 Planning and programming of the next stage

3.5 Conclusions

Bibliography

[1] Jacobs Wind Electric. [Online] Retrieved from http://www.jacobswind.net/ [Acccessed: 14/03/2019].

[2] Wind Charger. [Online] Retrieved from http://www.windcharger.org/Wind_Charger/Parris-Dunn_Corp..html [Acccessed: 14/03/2019].

[3] Bornay. [Online] Retrieved from https://www.bornay.com/es [Acccessed: 14/03/2019].

[4] B. Sanz, J. Ignacio Cruz, F. Javier España, P. Solanilla, A. Ponce, and A. García, *Guía sobre Tecnología Minieólica.* Madrid: Fenercom, Comunidad de Madrid, 2012.

[5] *Wind turbines – Part 2: Small wind turbines.* International Electrotechnical Commission 61400-2:2016.

[6] *Plan de Energías Renovables.* Madrid: Instituto Para la Diversificación y Ahorro de la Energía, 2011.

[7] A. Ghani Aissaoui and A. Tahour, *Wind Turbines: Design, Control and Applications.* IntechOpen, 2016.

[8] F. X. Sanz Cano, *Wind Turbines Design.* [Class Lecture] Terrassa: Escola Superior d'Enginyeries Industrial, Aeroespacial i Audiovisual de Terrassa, Universitat Politècnica de Catalunya, 2018.

[9] T. Burton, N. Jenkins, D. Sharpe, and E. Bossanyi, *Wind Energy Handbook.* Chichester: Wiley, 2011.

[10] Y. Oyha and T. Karasudani, "A shrouded wind tubine generating high output power," *Energies*, no. 4, pp. 634–649, 2012.

[11] Dromstorre. [Online] Retrieved from http://dromstore.dk [Acccessed: 02/04/2019].

[12] Enair. [Online] Retrieved from https://www.enair.es/ [Acccessed: 25/03/2019].

[13] SD Wind Energy. [Online] Retrieved from https://sd-windenergy.com/ [Acccessed: 25/03/2019].

[14] Smarttwister. [Online] Retrieved from http://www.smarttwister.org/ [Acccessed: 25/03/2019].

[15] Aeolos. [Online] Retrieved from http://www.windturbinestar.com/ [Acccessed: 25/03/2019].

[16] Bergey. [Online] Retrieved from http://bergey.com/ [Acccessed: 25/03/2019].

[17] Automaxx. [Online] Retrieved from https://autowindmill.weebly.com/windmill.html [Acccessed: 25/03/2019].

[18] Marsrock 400w economy windmill sale web page. [Online] Retrieved from https://www.amazon.com/MarsRock-Turbine-Generator-Economy-Windmill/dp/B077GS8Q4Z?psc=1&SubscriptionId=AKIAI3ZSW3WBYDZI6IPQ&tag=semprius-20&linkCode=xm2&camp=2025&creative=165953&creativeASIN=B077GS8Q4Z [Acccessed: 25/03/2019].

[19] D. Wood, *Small Wind Turbines: Analysis, Design and Application.* London: Springer, 2011.

[20] V. S. Fuentes, C. Troya, G. Moreno, and J. Molina, "Airfoil selection methodology for small wind turbines," *International Journal of Renewable Energy Research*, vol. 6, no. 4, pp. 1410–1415, 2016.

[21] XFOIL 6.9 Documentation. [Online] Retrieved from http://web.mit.edu/drela/Public/web/xfoil/xfoil_doc.txt [Acccessed: 15/05/2019].

[22] Airfoil tools. [Online] Retrieved from https://www.airfoiltools.com [Acccessed: 03/05/2019].

[23] University of Illinois in Urbana Champaign (UIUC) airfoil coordinates database. [Online] Retrieved from https://m-selig.ae.illinois.edu/ads/coord_database.html [Acccessed: 03/05/2019].

[24] H. Shah, N. Bhattarai, C. Lim, and S. Mathew, "Low Reynolds number airfoil for small horizontal axis wind turbine blades," *Sustainable future energy*, 2012.

[25] F. X. Sanz Cano, *Wind Turbines Design.* [Class Lecture] Terrassa: Escola Superior d'Enginyeries Industrial, Aeroespacial i Audiovisual de Terrassa, Universitat Politècnica de Catalunya, 2018.

[26] Small wind turbine contest. [Online] Retrieved from https://www.hanze.nl/nld/onderwijs/techniek/instituut-voor-engineering/organisatie/contest/international-small-wind-turbine-contest [Acccessed: 12/09/2019].